# Electron Trap to Electron Storage Center in Specially Aligned Mn- Doped CdSe d-Dot: A Step Forward in the Design of Higher Efficient Quantum-Dot Solar Cell

**ARTICLE** *in* JOURNAL OF PHYSICAL CHEMISTRY LETTERS · JULY 2014

Impact Factor: 7.46 · DOI: 10.1021/jz5012719



**4 AUTHORS:**

Tushar Debnath
Department of Atomic Energy
**17** PUBLICATIONS **55** CITATIONS
SEE PROFILE

Partha Maity
Bhabha Atomic Research Centre
**17** PUBLICATIONS **55** CITATIONS
SEE PROFILE

Maiti Sourav
Texas A&M University
**9** PUBLICATIONS **75** CITATIONS
SEE PROFILE

Hirendra N Ghosh
Bhabha Atomic Research Centre
**127** PUBLICATIONS **3,859** CITATIONS
SEE PROFILE

THE JOURNAL OF PHYSICAL CHEMISTRY Letters

Letter

pubs.acs.org/JPCL

# Electron Trap to Electron Storage Center in Specially Aligned Mn-Doped CdSe d-Dot: A Step Forward in the Design of Higher Efficient Quantum-Dot Solar Cell

Tushar Debnath, Partha Maity, Sourav Maiti, and Hirendra N. Ghosh*

Radiation & Photochemistry Division, Bhabha Atomic Research Centre, Trombay, Mumbai 400085, India

Supporting Information

**ABSTRACT:** Specially aligned surface-accumulated Mn-doped CdSe (MnCdSe) quantum dots (QDs) have been synthesized to study the effect of dopant atom on charge-carrier dynamics in QD materials. EPR studies suggest that the $^4T_1$ state of $Mn^{2+}$ lies above the conduction band of CdSe, and as a result no Mn-luminescence was observed from MnCdSe. Femtosecond transient absorption studies suggest that Mn atom introduces structural defects in surface-doped CdSe, which acts as electron trap center in doped QD for the photoexcited electron. Bromo-pyrogallol red (Br-PGR) were found to form strong charge-trasfer complex with both CdSe and MnCdSe QDs. Charge separation in both the CdSe/Br-PGR and MnCdSe/Br-PGR composites was found to take place in three different pathways by transferring the photoexcited hole of CdSe/MnCdSe QDs to Br-PGR, electron injection from photoexcited Br-PGR to the QDs, and direct electron transfer from the HOMO of Br-PGR to the conduction band of both the QDs. Hole-transfer dynamics are found to be quite similar (~1.1 to 1.3 ps) for both of the systems and found to be independent of Mn doping. However, charge recombination dynamics was found to be much slower in the MnCdSe/Br-PGR system as compared with that in the CdSe/Br-PGR system, which confirms that the Mn dopant act as the electron storage center. As a consequence, the MnCdSe/Br-PGR system can be used as a better super sensitizer in quantum-dot-sensitized solar cell to increase efficiency further.

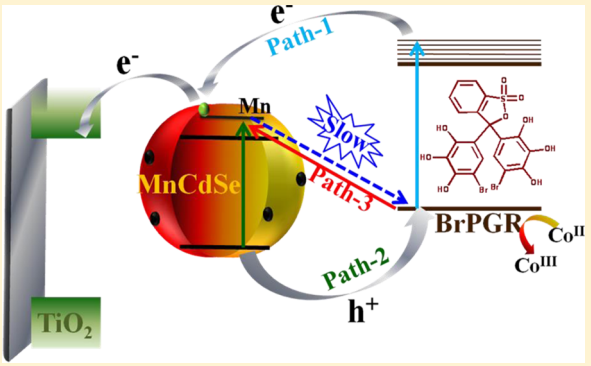


**SECTION:** Physical Processes in Nanomaterials and Nanostructures

Quantum dots (QDs) have drawn attention in the contemporary research areas due to their band-gap tunability and multiexciton generation (MEG), and effortless synthesis makes them efficient candidates for quantum-dot solar cell (QDSC).[1−12] Now introduction of dopant (impurities) materials in these quantum dots and semiconductors is widely used to modify the intrinsic properties of host semicondutor nanocrystals such as electrical conductivity and magnetic properties.[13−16] Doping of the QDs with paramagnetic transition-metal ions (Mn, Cu, etc.) have become more interesting because the dopant materials can tune optical properties and magnetic properties and also act as photoluminescence activator.[17−20] Doping of 3d transition metal such as Mn in II−VI semiconductor quantum dots (QDs) have been widely investigated for very high Mn-emission quantum yield (QY)[21] and long emission lifetime for energy storage.[22−24] In general, QDs have strong photoluminescence in the spectrum region of blue to red depending on size and shape of the particles. The photoluminescence property of Mn-doped QDs were found to change drastically due to the presence of atomic-like Mn d-emission that arises due to $^4T_1$-$^6A_1$ transition.[13,22,25] The transition between $^4T_1$-$^6A_1$ is both spin and orbitally forbidden as a result emission lifetime measured to be in the range of milliseconds.[15] Long excited-state lifetime is one of the key factors for the design and development of higher efficient QDSC. Recently Kamat and coworkers[26] have reported over 5% efficiency for Mn-doped CdS/CdSe QDSC and attributed the Mn atom to play a major role for the improvement. However, the effect of dopant materials on the excited-state dynamics and charge-carrier dynamics in ultrafast time scale of QD materials is not reported in literature. Although Mn-doped QDs were found to be better materials for conversion of solar energy, real mechanisms of such improvement are never discussed in the literature. To understand the effect of dopant atom on both optical and sensitization properties of QD materials, it is very important to monitor the excited-state properties on the ultrafast time scale.

To understand the previously unexplained facts of doped QDs, we have synthesized Mn-doped CdSe QDs named MnCdSe. To compare the properties of MnCdSe, undoped CdSe QD also has been synthesized and characterized by steady-state absorption and luminescence studies. Femtosecond transient absorption measurements have been carried out by

**Received:** June 21, 2014
**Accepted:** July 31, 2014

   dx.doi.org/10.1021/jz5012719 | J. Phys. Chem. Lett. 2014, 5, 2836−2842

exciting both CdSe and MnCdSe and monitoring the transients in Vis-near IR region on the ultrafast times scale. Carrier cooling and charge recombination (CR) dynamics have been compared for both the doped and undoped one. In addition to that another organic molecule, bromo-pyrogallol red (Br-PGR) has been used as the supersensitized adsorbate on both the QD particles, and charge-transfer dynamics have been demonstrated on the ultrafast time scale, where Br-PGR forms a strong charge-transfer (CT) complex with both CdSe and MnCdSe.

Mn-doped CdSe QD was synthesized by adopting previously reported high-temperature hot injection method with some modifications.[25,27] Steady-state optical absorption studies show excitonic absorption peak at ~520 nm and emission peak at 560 nm for MnCdSe QD in Figure 1. Emission QY was

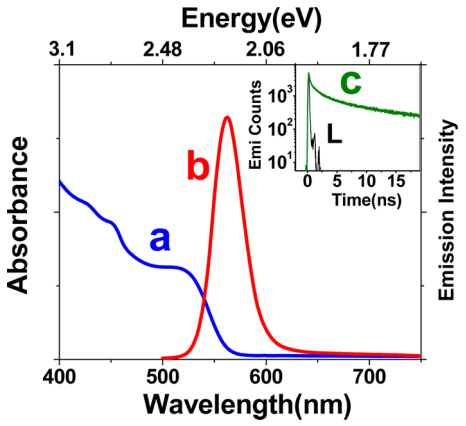


**Figure 1.** Steady-state (a) optical absorption spectrum and (b) luminescence spectrum of MnCdSe QD. Inset: (c) Time-resolved emission decay trace of MnCdSe QD at 560 nm after exciting at 490 nm. L stands for lamp profile of 490 nm laser excitation source.

determined to be 5.5%. We have also synthesized undoped CdSe QD and found it to emit at 550 nm with 10% emission QY. Mn d-emission due to atomic like $^4T_1$-$^6A_1$ transition appears at 590 nm (~2.1 eV).[26] However, we have observed marginal change in emission wavelength in MnCdSe as compared with CdSe QD, and the shape of both spectra are similar in nature. To confirm that luminescence at 560 nm for MnCdSe QD is purely due to excitonic emission, we have carried out delayed photoluminescence measurements, and results are shown in the Supporting Information. No luminescence has been observed after 100 $\mu$s delay (SI Figure 2). So we can conclude that emission that appeared in MnCdSe is solely due to excitonic emission of CdSe and not from $^4T_1$-$^6A_1$ transition. Again excitonic emission lifetime for

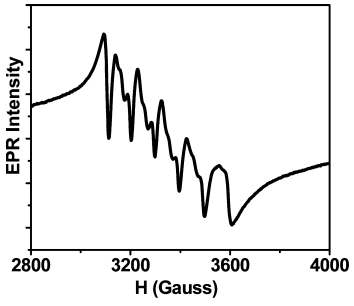


**Figure 2.** Electron paramagnetic resonance spectrum of Mn-doped CdSe QD. Hyperfine constant ($A$) is found to be ~89 × $10^{-4}$ $cm^{-1}$.

MnCdSe QD was measured to be 2.2 ns (Figure1 inset), which is much shorter as compared with Mn d-emission.[15] The emission lifetime for undoped CdSe was determined to be 2.1 ns. Previously Gamelin and coworkers[15,22] suggested that if the particle size of Mn-doped CdSe is bigger than 3.3 nm, then no Mn-luminescence can be observed from the doped particle. They have suggested that Mn d-emission can be completely diminished by tuning the size of doped particle.[15,22] It has been shown that when the size of CdSe QD is >3.3 nm, the conduction band (CB) of CdSe lies below the $^4T_1$ state of Mn (Scheme 1); as a result, only excitonic emission due to CdSe

**Scheme 1. Schematic Diagram Showing Disappearance of Mn-Luminescence with Increasing CdSe Diameter (>3.3 nm) (adopted from Gamelin and coworkers[22])**

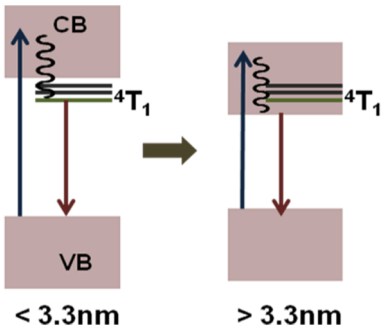


QD is observed.[22] However, in the present investigation, particle sizes were determined to be 2.8 nm by sizing curve analysis from excitonic absorption and HRTEM measurements (Supporting Information). In that case, Mn luminescence is expected from the 2.8 nm MnCdSe QD. At this juncture, we would like to clarify that in the case of undoped wide band gap QDs (CdS, ZnS),[16,21] due to size variation one can observe tunable excitonic emission; however, in the case of Mn-doped QDs due to the presence of strong Mn-luminescence, emission is unaffected by size variation of doped QD. Previously, Pradhan and Peng[25] and Pradhan and Sarma[16] have shown that Mn-doped ZnSe has much less tunability (<150 meV) in photoluminescence. However, very recently Sarma and coworkers have demonstrated that Mn d-emission can be tunable to wider range in Mn-doped $Zn_{0.25}Cd_{0.75}S$ alloyed NC[28] as well as Mn-doped ZnSe/CdSe/ZnSe QDs.[29] Such a wider tunable luminescence has been explained on the basis of variation of ligand field splitting, which is associated with the large number of inequivalent sites for doped Mn atom in QD materials[28] and due to strain in the interface of QD core−shell.[29] Now to confirm Mn doping in the present investigation, electron paramagnetic resonance (EPR) measurements for the newly synthesized MnCdSe QD have been carried out. Figure 2 shows the EPR pattern of Mn-doped CdSe QD particle, which clearly indicates that Mn resonance is split into six lines due to hyperfine coupling of five unpaired electrons in Mn. The hyperfine constant ($A$) is found to be ~89 × $10^{-4}$ $cm^{-1}$ for MnCdSe QD. Such high value of $A$ indicates that most of the dopants atoms (Mn) reside near the surface layer of the crystal structure of CdSe QD. If Mn would reside in the core of the nanocrystal, then typical $A$ should be in the range of ~65 × $10^{-4}$ $cm^{-1}$.[13,30,31] It is reported in the literature that at such high $A$ value the Mn atom exists as isolated $Mn^{2+}$ ions on the surface.[32,33] Thus, such high $A$ value can exclude the option for the formation of $MnSe_2$ (or similar) compound. Santra et al.[26]


dx.doi.org/10.1021/jz5012719 | J. Phys. Chem. Lett. 2014, 5, 2836−2842

have demonstrated that ligand field splitting progressively increases from core-accumulated Mn to the surface-accumulated Mn-doped QD. They have shown that one can tune the Mn d-emission to a large extent, that is, 1.97 (630 nm) to 2.34 eV (530 nm). So schematically we can visualize the energy splitting in core and surface, as shown in Scheme 2.

**Scheme 2. Alignment of Energy Level of Mn-Doped CdSe Quantum Dot Where Mn Atom Resides in Core of the QD and Surface of the QD[a]**

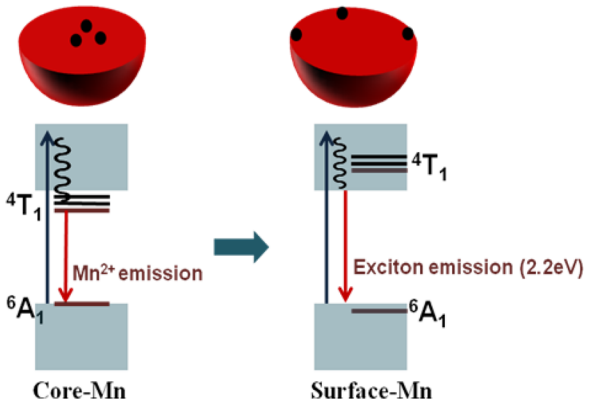


[a]Schematic diagram showing that ligand field splitting of Mn increases from core to surface of QD materials. EPR studies and presence of band-edge emission of CdSe suggest Mn atoms are localized in the surface of QD in the present studies.

As the excitonic emission of MnCdSe appeared at 560 nm (~2.2 eV) it can be concluded that $^4T_1$ state of Mn will lie above than CB edge of CdSe QD, as shown in Scheme 2. Due to such alignment in MnCdSe QD of 2.8 nm particle, no Mn-luminescence has been observed in the present investigation. To the best of our knowledge, we are reporting such behavior of Mn-doped CdSe QD for the first time in literature. Now it is very important to know the effect of doping in MnCdSe on charge-carrier dynamics on an ultrafast time scale in the present studies. To understand carrier cooling, surface trapping and CR behavior in ultrafast time scale for both CdSe and MnCdSe QDs, we have carried out femtosecond transient absorption spectroscopic measurements after exciting the sample at 400 nm laser light. Figure 3A,B shows the transient absorption spectrum of CdSe QD and MnCdSe QD at different time delay. In both of the systems, broad negative absorption is observed in the 480−560 nm region, which can be attributed to excitonic (1S exciton) bleach. In addition to that, negligible positive absorption was observed in the range of the 560−720 nm region, which indicates the presence of fewer surface defect states in both CdSe QDs and MnCdSe QDs. Broadening in excitonic bleach of MnCdSe as compared with CdSe excitonic bleach is consistent with their optical absorption spectrum. The inset in Figure 3A,B shows the bleach recovery kinetics at 530 nm for CdSe and 530 nm for MnCdSe, respectively. The bleach recovery kinetics can be fitted with double-exponential growth and multiexponential recovery with different time constants and is shown in Table 1. The second growth time constants at the bleach wavelength in transient absorption measurements are attributed to cooling dynamics of photoexcited electron.[34] Interestingly, the carrier cooling dynamics were found to be faster (500 fs) in MnCdSe as compared with CdSe QD (600 fs) (Table1). This might be due to the presence of $^4T_1$ states of

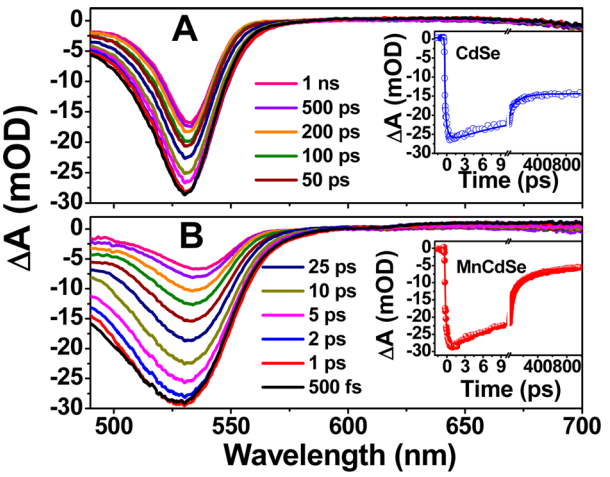


**Figure 3.** Transient absorption spectrum of (A) CdSe QD and (B) MnCdSe QD in chloroform at different time delay after exciting the sample at 400 nm laser light. Inset: Bleach recovery kinetics at 530 nm of CdSe QD (A) and at 530 nm for MnCdSe (B) is shown.

Mn, which are overlapped with CB states and facilitated electron cooling process. It is very interesting to see that for MnCdSe QD the bleach recovery kinetics becomes faster as compared with CdSe QD. Recently Son and coworkers[24] reported faster bleach recovery (CR) for Mn-CdSe/ZnS-doped nanocrystals as compared with that of undoped particles and endorsed that this was due to the creation of additional charge-carrier traps (viz. electron trap). Similarly, in the present investigation, we can also conclude that in the MnCdSe QD, CR is faster due to the presence of Mn-doped related electron trap center.

However, the main aim of this investigation is how Mn-doped CdSe (MnCdSe) QDs can behave as supersensitizer as compared with CdSe QDs for the application in QDSC. Many others including our group have previously demonstrated[35−41] that in supersensitized QD (CdSe, CdS) composite materials, both QD and molecular adsorbate, cosensitized $TiO_2$ electrode where the photoexcited hole from QD can be captured by molecular adsorbate and also photoexcited molecular adsorbate can inject electron into the QD, resulting grand charge separation in the composite system. So it is very important to know how MnCdSe behaves as a supersensitizer material in the presence of a suitable molecular adsorbate, where the Mn atom acts as an electron storage center. The CT complex formation in the ground state between QD and molecular adsorbate and their consequences in CT (both hole/electron) behavior in the ultrafast time domain have not been widely investigated, except in our very recent work.[35,36] In the present investigation, we have chosen bromo pyrogallol red (BrPGR) molecule as the sensitizer to QD (both CdSe and MnCdSe), which has both HOMO and LUMO above the valence band (VB) and CB of the QD materials (Scheme 3). Figure 4 shows the optical absorption spectra of pure CdSe and MnCdSe QDs, Br-PGR, and their composite mixture. It is clear that both CdSe and MnCdSe QDs form a strong CT complex with Br-PGR with the emergence of a new CT band in the entire visible region (up to 800 nm), where both Br-PGR and QDs (both CdSe and MnCdSe) absorb below the 600 nm region. BrPGR has an optical absorption maxima at 482 nm, whereas CdSe has the first excitonic peak at ~520 nm. However, the CdSe/Br-PGR composite mixture shows optical absorption beyond 800 nm


dx.doi.org/10.1021/jz5012719 | J. Phys. Chem. Lett. 2014, 5, 2836−2842

**Table 1. Kinetic Fitting Parameters at Excitonic Bleach Position for CdSe QD and MnCdSe QD after 400 nm Laser Excitation[a]**

| system/probe wavelength | $\tau_{growth}^{1}$ | $\tau_{growth}^{2}$ | $\tau_1$ | $\tau_2$ | $\tau_3$ |
|---|---|---|---|---|---|
| CdSe/530 nm | <100 fs (90%) | 600 fs (10%) | 14 ps (32.8%) | 140 ps (11.2%) | >1 ns (56%) |
| MnCdSe/530 nm | <100 fs (84%) | 500 fs (16%) | 15 ps (54.7%) | 180 ps (23.9%) | >1 ns (21.4%) |

[a]Numbers in the parentheses are the pre-factors that indicate the percentage of decay (or growth) with that time constant.

**Scheme 3. Schematic Diagram Illustrating Electron Injection and Hole Transfer Process in MnCdSe/Br-PGR Composite[a]**

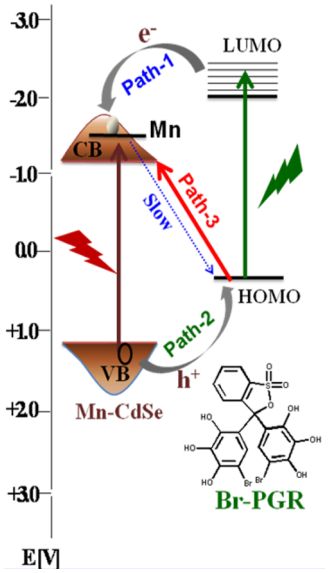


[a]Structure of Br-PGR molecule has also been shown.

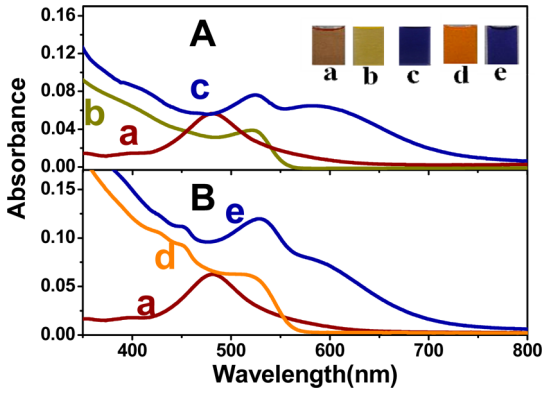


**Figure 4.** (A) Steady-state optical absorption spectra of (a) Br-PGR molecule, (b) CdSe QD, and (c) CdSe/Br-PGR composite in chloroform. (B) Steady-state optical absorption spectra of (a) Br-PGR molecule, (d) Mn-doped CdSe d-Dot, and (e) Mn-doped CdSe/Br-PGR composite in chloroform. Inset A: Color of different sample solutions in chloroform.

with optical absorption maxima at ~525 nm and a broad hump at 590 nm (Figure 4A). In MnCdSe QDs, the first excitonic peak appears at ~520 nm. The composite mixture of MnCdSe/Br-PGR shows optical absorption maxima at ~530 nm, with a broad hump at ~600 nm (Figure 4B). It is clearly visible from optical absorption studies that the shape of CT absorption spectra for the above composite materials are little different. In the case of the MnCdSe/Br-PGR system, the CT absorption band is a little red-shifted, and also molecular absorptivity is higher as compared with that of CdSe/Br-PGR system. We contemplate that this is due to the involvement of Mn states, which energetically lies above the CB edge. Benesi–Hildebrand (BH) plots for both composite systems have been carried out and are shown in the Supporting Information. The equilibrium constant was calculated to be ~$1.2 \times 10^8$ $M^{-1}$ for CdSe/BrPGR super sensitizer and $1.5 \times 10^8$ $M^{-1}$ for MnCdSe/BrPGR super sensitizer. Steady-state and time-resolved emission spectroscopic measurements have been carried out for both of the previously described composite systems and also free QDs, which confirms that the photoexcited holes from both CdSe and MnCdSe QDs were very efficiently captured by Br-PGR (Supporting Information).

Now to comprehend the charge-transfer (both electron and hole) dynamics in both CdSe/BrPGR and MnCdSe/BrPGR composite systems in ultrafast time scale, we have carried out femtosecond transient absorption spectroscopy after exciting the sample at 400 nm laser light. The transient absorption spectral and kinetic behaviors of both CdSe QD and MnCdSe d-dot sensitized with BrPGR molecule are quite similar. Both of the transient spectra contain sharp bleach in 480–560 nm region and broad bleach (less intense) in the 560–720 nm region (Figure 5). The negative absorption in the blue region of

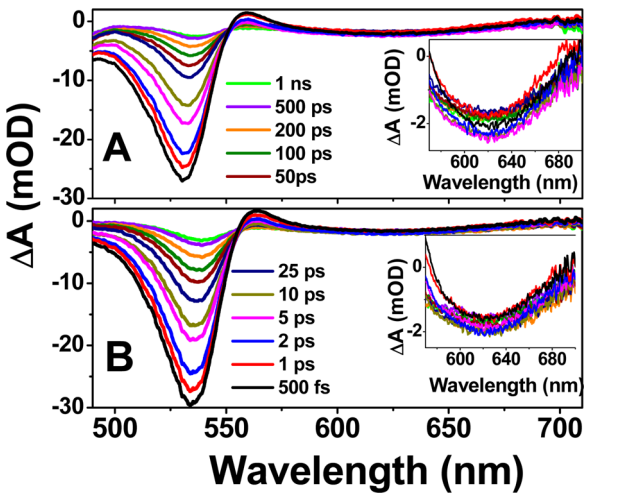


**Figure 5.** Transient absorption spectra of (A) CdSe/Br-PGR and (B) MnCdSe/Br-PGR composite materials in chloroform at different time delay after excitation at 400 nm laser light. (Inset) Expanded view of the transient spectra of (A) CdSe/Br-PGR and (B) MnCdSe/Br-PGR composite materials in 570–700 nm region.

the spectra can be attributed to excitonic bleach for the QDs and the broad negative absorption in the red region of the spectra can be attributed to bleach due to the charge-separated complex. It is interesting to see that bleach intensity due to CT absorption band is much less as compared with the excitonic bleach for both the composite systems. This might be due to the 400 nm laser excitation majority of the light absorbed by the QD (CdSe or MnCdSe) materials as compared with that of CT complex. As a result, the bleach intensity of the CT band becomes very less as compared with exciton bleach of QDs. It is reported in the literature that photoexcitation of heteronanos-


dx.doi.org/10.1021/jz5012719 | J. Phys. Chem. Lett. 2014, 5, 2836–2842

tructure materials like CdSe/CdTe nanorod[42] and ZnSe/CdS/Pt[43] composite materials also show bleach due to CT absorption in addition to the excitonic bleach of the QD materials. Although from steady-state and time-resolved studies, we have confirmed that on photoexcitation of QDs/Br-PGR composite mixtures both electron injection and hole transfer take place; however, no signature of cation radical was observed, unlike our previous investigations on QD/dye composite materials.[35,37] This might be due to a huge overlap of transient band due to cation radical of molecular adsorbate (BrPGR) and ground-state bleach for the CT complex. Although no absorption due to cation radical was observed; however, transient absorption spectra of the composite materials (Figure 5) are quite different from the pure QD materials (Figure 3) and Br-PGR (Supporting Information), suggesting interfacial charge exchange between QDs (both CdSe and MnCdSe) and Br-PGR. To understand CT dynamics, we have monitored the bleach recovery kinetics at both excitonic wavelengths (530 nm for CdSe and 535 nm for MnCdSe) and at the bleach maxima of the complexes, as shown in Figure 6. The recovery kinetics at excitonic wavelengths can

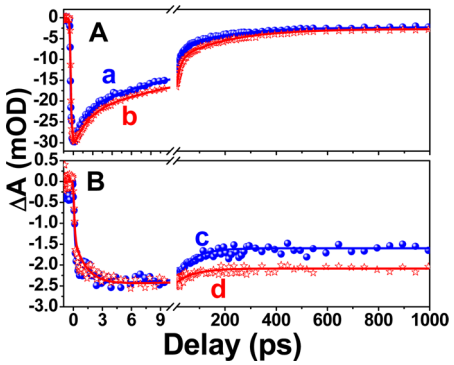


**Figure 6.** (A) Bleach recovery kinetics of (a) CdSe/Br-PGR complex at 530 nm and (b) MnCdSe/Br-PGR complex at 535 nm. (B) Bleach recovery kinetics of (c) CdSe/Br-PGR complex at 625 nm and (d) MnCdSe/Br-PGR complex at 630 nm after exciting with 400 nm laser light.

be fitted with single exponential growth and multiexponential recovery components (Table 2). In both cases, we have observed pulse-width-limited growth (<100 fs) and multiexponential recovery with time constants of $\tau_1$ = 1.1 ps (40%), $\tau_2$ = 15 ps (41%), $\tau_3$ = 200 ps (11%), and $\tau_4$ = >1 ns (8%) for the CdSe/Br-PGR system and $\tau_1$ = 1.3 ps (36.5%), $\tau_2$ = 15 ps (39%), $\tau_3$ = 200 ps (16%), and $\tau_4$ = >1 ns (8.5%) for the MnCdSe/Br-PGR system (Table 2). It is interesting to see that the majority of the bleach at excitonic wavelength recovers 1.1 to 1.3 ps in both composite systems, whereas the first bleach recovery time constants are 14 to 15 ps for both pure QDs (Figure 3, Table 1). We are attributing this 1.1 to 1.3 ps component as hole transfer from photoexcited QD to Br-PGR in both systems. In our previous investigation in CdS/dibromo fluorescein (DBF) and CdSe/aurin tricarboxylic acid (ATC) super-sensitized systems, hole transfer time was determined from the faster component of the bleach recovery kinetics and determined to be 800 fs for CdS/DBF system[35] and 900 fs and 3 ps for the CdSe/ATC system.[36] It is interesting to see that hole-transfer times in both CdSe/Br-PGR and MnCdSe/Br-PGR are very similar (1.1 to 1.3 ps). This observation clearly indicates that there is no effect of Mn doping on QD materials on hole-transfer dynamics. The bleach recovery kinetics at excitonic wavelength was dominated by the hole-transfer process, so to find out the CR dynamics bleach recovery kinetics at the maxima of CT complex bleach were monitored. Bleach recovery kinetics at 625 nm for CdSe/Br-PGR can be fitted by biexponential growth with time constants of $\tau_1^g$ = < 100 fs (80%) and $\tau_2^g$ = 1.1 ps (20%) and by biexponential recovery with time constants of $\tau_1$ = 60 ps (33%) and $\tau_2$ = >1 ns (67%). The kinetics at 630 nm for MnCdSe/Br-PGR can be fitted by biexponential growth with time constants of $\tau_1^g$ = < 100 fs (75%) and $\tau_2^g$ = 1.3 ps (25%) and by biexponential recovery with time constants of $\tau_1$ = 70 ps (14%) and $\tau_2$ = >1 ns (86%). It is interesting to see that growth at the bleach maxima can be fitted biexponentially in both the systems, which can be attributed to charge-separation time. In the present investigation, we have carried out transient absorption measurements after exciting the samples at 400 nm in which pure QDs, Br-PGR and also CT complex can be excited. On photoexcitation with 400 nm laser light, the charge separation can take place in three different pathways, as shown in Scheme 3. We have observed in our previous investigation[36,37] that photoexcited PGR and ATC (another class of TPM dyes[44,45]) inject electron in the CB in pulse-width limited time (<100 fs). Similarly, in the present investigation, photoexcited Br-PGR can also inject electron in <100 fs, which we can attribute to path 1 (Scheme 3). We have already observed that hole transfer can take place from photoexcited QDs to Br-PGR with the time range of 1.1 to 1.3 ps for both the systems, which can be attributed to path 2 (Scheme 3), which exactly matches with second growth time (Table 2). Finally, charge separation can also take place by exciting the CT complex, where electron from the Br-PGR HOMO level directly transfers to the CB of QDs that take place in <100 fs (pulse width time), which is attributed to path 3 (Scheme 3). Finally, the CR reaction has been monitored by following the bleach recovery time at 625/630 nm, and we found that in the MnCdSe/Br-PGR system the CR reaction is much slower as compared with that in the CdSe/Br-PGR system. Here $^4T_1$ states of MnCdSe act as the electron storage center for the electron in the CB. Slower CR in MnCdSe/Br-PGR composite will, in turn, improve the efficiency of supersensitized QDSC.

**Table 2. Kinetic Fitting Parameters at Different Wavelengths for the Transients of CdSe/Br-PGR and MnCdSe/Br-PGR Composites after 400 nm Laser Excitation[a]**

| system/$\lambda_{probe}$ | $\tau_{growth}^1$ | $\tau_{growth}^2$ | $\tau_1$ | $\tau_2$ | $\tau_3$ | $\tau_4$ |
|---|---|---|---|---|---|---|
| CdSe-BrPGR/530 nm | <100 fs | | 1.1 ps (40%) | 15 ps (41%) | 200 ps (11%) | >1 ns (8%) |
| MnCdSe-BrPGR/535 nm | <100 fs | | 1.3 ps (36.5%) | 15 ps (39%) | 200 ps (16%) | >1 ns (8.5%) |
| CdSe-BrPGR/625 nm | <100 fs (80%) | 1.1 ps (20%) | 60 ps (33%) | >1 ns (67%) | | |
| MnCdSe-BrPGR/630 nm | <100 fs (75%) | 1.3 ps (25%) | 70 ps (14%) | >1 ns (86%) | | |

[a]Numbers in the parentheses are the pre-factors that indicate the percentage of decay (or growth) with that time constant.


dx.doi.org/10.1021/jz5012719 | J. Phys. Chem. Lett. 2014, 5, 2836−2842

In summary, we have synthesized surface-accumulated Mn-doped CdSe d-dot with a special type of alignment, where $^4T_1$ states of Mn atom lie above the CB of-doped CdSe. The presence of Mn atom in the surface of doped QD was confirmed by EPR studies. Cooling dynamics of photoexcited charge carrier was found to be faster in doped QD as compared with that in the undoped QD. Both undoped and Mn-doped CdSe QDs were found to form strong charge-transfer complex with Br-PGR and the composite materials can act as a supersensitizer where the CT complexes absorb more solar radiation as compared with both QDs and Br-PGR. Charge separations in both of the composite materials were found to take place by transfer of the photoexcited hole of CdSe/MnCdSe QDs to Br-PGR, electron injection from photoexcited Br-PGR to the QDs, and direct electron transfer from the HOMO of Br-PGR to the CB of both the QDs. Hole transfer was found to take place in 1.1 to 1.3 ps in the previously described systems, and electron injection from photoexcited Br-PGR to QDs and direct electron transfer from the HOMO level of Br-PGR to the CB of QDs were found to take place on the <100 fs time scale after exciting the sample at 400 nm laser light. CR time was found to be much slower in the MnCdSe/Br-PGR system due to the presence of Mn dopant (act as electron storage center) as compared with that of the CdSe/Br-PGR system and can act as a better super sensitizer materials for the development of higher efficient QDSC.

## ■ ASSOCIATED CONTENT

### Supporting Information

Details of the synthesis of CdSe quantum dot and Mn-doped CdSe d-dot, HRTEM image, delayed PL measurement, Benesi−Hildebrand (BH) plot, luminescence quenching experiments for both CdSe/Br-PGR and MnCdSe/Br-PGR composite, and experimental setup for transient absorption measurements. This material is available free of charge via the Internet at http://pubs.acs.org.

## ■ AUTHOR INFORMATION

### Corresponding Author

*E-mail: hnghosh@barc.gov.in. Fax: (+) 91-22-25505331/25505151.

### Notes

The authors declare no competing financial interest.

## ■ ACKNOWLEDGMENTS

This work was supported by "DAE-SRC Outstanding Research Investigator Award" (Project/Scheme No.: DAE-SRC/2012/21/13-BRNS) granted to Dr. H. N. Ghosh. T.D. acknowledges CSIR and P.M. acknowledges DAE for research fellowship. We sincerely thank Dr. R. M. Kadam, Radiochemistry Division, BARC. We also acknowledge Dr. D. K. Palit and Dr. B. N. Jagatap for their encouragement.

## ■ REFERENCES

(1) Kamat, P. V. Quantum Dot Solar Cells. Semiconductor Nanocrystals as Light Harvesters. *J. Phys. Chem. C* **2008**, *112*, 18737−18753.

(2) Kamat, P. V. Quantum Dot Solar Cells. The Next Big Thing in Photovoltaics. *J. Phys. Chem. Lett.* **2013**, *4*, 908−918.

(3) Palomares, E.; Martinez-Ferrero, E.; Albero, J. Materials, Nanomorphology and Interfacial Charge Transfer Reactions in Quantum Dot/Polymer Solar Cell Devices. *J. Phys. Chem. Lett.* **2010**, *1*, 3039−3045.

(4) Huang, J.; Huang, Z.; Yang, Y.; Zhu, H.; Lian, T. Multiple Exciton Dissociation in CdSe Quantum Dots by Ultrafast Electron Transfer to Adsorbed Methylene Blue. *J. Am. Chem. Soc.* **2010**, *132*, 4858−4864.

(5) Song, N.; Zhu, H.; Jin, S.; Lian, T. Hole Transfer from Single Quantum Dots. *ACS Nano* **2011**, *5*, 8750−8759.

(6) Robel, I.; Subramanian, V.; Kuno, M.; Kamat, P. V. Quantum Dot Solar Cells. Harvesting Light Energy with CdSe Nanocrystals Molecularly Linked to Mesoscopic TiO2 Films. *J. Am. Chem. Soc.* **2006**, *128*, 2385−2393.

(7) Ellingson, R. J.; Beard, M. C.; Johnson, J. C.; Yu, P.; Micic, O. I.; Nozik, A. J.; Shabaev, A.; Efros, A. L. Highly Efficient Multiple Exciton Generation in Colloidal PbSe and PbS Quantum Dots. *Nano Lett.* **2005**, *5*, 865−871.

(8) Luther, J. M.; Beard, M. C.; Song, Q.; Law, M.; Ellingson, R. J.; Nozik, A. J. Multiple Exciton Generation in Films of Electronically Coupled PbSe Quantum Dots. *Nano Lett.* **2007**, *7*, 1779−1784.

(9) Schaller, R. D.; Klimov, V. I. High Efficiency Carrier Multiplication in PbSe Nanocrystals: Implications for Solar Energy Conversion. *Phys. Rev. Lett.* **2004**, *92*, 186601.

(10) Schaller, R. D.; Sykora, M.; Pietryga, J. M.; Klimov, V. I. Seven Excitons at a Cost of One: Redefining the Limits for Conversion Efficiency of Photons into Charge Carriers. *Nano Lett.* **2006**, *6*, 424−429.

(11) Beard, M. C.; Luther, J. M.; Semonin, O. E.; Nozik, A. J. Third Generation Photovoltaics based on Multiple Exciton Generation in Quantum Confined Semiconductors. *Acc. Chem. Res.* **2013**, *46*, 1252−1260.

(12) Klimov, V. I. Spectral and Dynamical Properties of Multiexcitons in Semiconductor Nanocrystals. *Annu. Rev. Phys. Chem.* **2007**, *58*, 635−673.

(13) Norris, D. J.; Efros, A. L.; Erwin, S. C. Doped Nanocrystals. *Science* **2008**, *319*, 1776−1779.

(14) Vlaskin, V. A.; Beaulac, R.; Gamelin, D. R. Dopant-Carrier Magnetic Exchange Coupling in Inverted Core/Shell Nanocrystals. *Nano Lett.* **2009**, *9*, 4376−4382.

(15) Vlaskin, V. A.; Janssen, N.; Rijssel, J. v.; Beaulac, R.; Gamelin, D. R. Tunable Dual Emission in Doped Semiconductor Nanocrystals. *Nano Lett.* **2010**, *10*, 3670−3674.

(16) Pradhan, N.; Sarma, D. D. Advances in Light-Emitting Doped Semiconductor Nanocrystals. *J. Phys. Chem. Lett.* **2011**, *2*, 2818−2826.

(17) Niladri, S. K.; Sarma, D. D.; Kadam, R. M.; Pradhan, N. Doping Transition Metal (Mn or Cu) Ions in Semiconductor Nanocrystals. *J. Phys. Chem. Lett.* **2010**, *1*, 2863−2866.

(18) Archer, P. I.; Santangelo, S. A.; Gamelin, D. R. Direct Observation of sp-d Exchange Interactions in Colloidal Mn2+- and Co2+-doped CdSe Quantum Dots. *Nano Lett.* **2007**, *7*, 1037−1043.

(19) Santangelo, S. A.; Hinds, E. A.; Vlaskin, V. A.; Archer, P. I.; Gamelin, D. R. Bimodal Bond-Length Distributions in Cobalt-Doped CdSe, ZnSe, and $Cd_{1-x}Zn_xSe$ Quantum Dots. *J. Am. Chem. Soc.* **2007**, *129*, 3973−3978.

(20) Panda, S. K.; Hickey, S. G.; Demir, H. V.; Eychmuller, A. Bright White-Light Emitting Manganese and Copper Co-Doped ZnSe Quantum Dots. *Angew. Chem.* **2011**, *123*, 4524−4528.

(21) Srivastava, B. B.; Jana, S.; Karan, N. S.; Paria, S.; Jana, N. R.; Sarma, D. D.; Pradhan, N. Highly Luminescent Mn-Doped ZnS Nanocrystals: Gram-Scale Synthesis. *J. Phys. Chem. Lett.* **2010**, *1*, 1454−1458.

(22) Beaulac, R.; Archer, P. I.; Ochsenbein, S. T.; Gamelin, D. R. $Mn^{2+}$-Doped CdSe Quantum Dots: New Inorganic Materials for Spin-Electronics and Spin-Photonics. *Adv. Funct. Mater.* **2008**, *18*, 3873−3891.

(23) Beaulac, R.; Archer, P. I.; van Rijssel, J.; Meijerink, A.; Gamelin, D. R. Exciton Storage by Mn2+ in Colloidal Mn2+-Doped CdSe Quantum Dots. *Nano Lett.* **2008**, *8*, 2949−2953.

(24) Chen, H. Y.; Maiti, S.; Son, D. H. Doping Location-Dependent Energy Transfer Dynamics in Mn-Doped CdS/ZnS Nanocrystals. *ACS Nano* **2012**, *6*, 583−591.

(25) Pradhan, N.; Peng, X. Efficient and Color-Tunable Mn-Doped ZnSe Nanocrystal Emitters: Control of Optical Performance via

Greener Synthetic Chemistry. *J. Am. Chem. Soc.* **2007**, *129*, 3339−3347.
(26) Santra, P. K.; Kamat, P. V. Mn-Doped Quantum Dot Sensitized Solar Cells: A Strategy to Boost Efficiency over 5%. *J. Am. Chem. Soc.* **2012**, *134*, 2508−2511.
(27) Qu, L.; Peng, X. Control of Photoluminescence Properties of CdSe Nanocrystals in Growth. *J. Am. Chem. Soc.* **2002**, *124*, 2049−2055.
(28) Hazarika, A.; Layek, A.; De, S.; Nag, A.; Debnath, S.; Mahadevan, P.; Chowdhury, A.; Sarma, D. D. Ultranarrow and Widely Tunable $Mn^{2+}$-Induced Photoluminescence from Single Mn-Doped Nanocrystals of ZnS-CdS Alloys. *Phys. Rev. Lett.* **2013**, *110*, 267401.
(29) Hazarika, A.; Pandey, A.; Sarma, D. D. Rainbow Emission from an Atomic Transition in Doped Quantum Dots. *J. Phys. Chem. Lett.* **2014**, *5*, 2208−2213.
(30) Kennedy, T. A.; Glaser, E. R.; Klein, P. B. Symmetry and electronic structure of the Mn impurity in ZnS nanocrystals. *Phys. Rev. B* **1995**, *52* (20), 356−359.
(31) Koh, A. K.; Miller, D. J. The Systematic Variation of the EPR Parameters of Manganese in II-VI Semiconductors. *Solid State Commun.* **1986**, *60* (3), 217−222.
(32) Magana, D.; Perera, S. C.; Harter, A. G.; Dalal, N. S.; Strouse, G. F. Switching-on Superparamagnetism in Mn/CdSe Quantum Dots. *J. Am. Chem. Soc.* **2006**, *128*, 2931−2939.
(33) Jing, L.; Ding, K.; Kalytchuk, S.; Wang, Y.; Qiao, R.; Kershaw, S. V.; Rogach, A. L.; Gao, M. Aqueous Manganese-Doped Core/Shell CdTe/ZnS Quantum Dots with Strong Fluorescence and High Relaxivity. *J. Phys. Chem. C* **2013**, *117*, 18752−18761.
(34) Rawalekar, S.; Kaniyankandy, S.; Verma, S.; Ghosh, H. N. Ultrafast Charge Carrier Relaxation and Charge Transfer Dynamics of CdTe/CdS Core-Shell Quantum Dots as Studied by Femtosecond Transient Absorption Spectroscopy. *J. Phys. Chem. C* **2010**, *114*, 1460−1466.
(35) Maity, P.; Debnath, T.; Ghosh, H. N. Ultrafast Hole and Electron Transfer Dynamics in CdS/Di-bromofluorescein (DBF) Super-Sensitized Quantum Dot Solar Cell Materials. *J. Phys. Chem. Lett.* **2013**, *4*, 4020−4025.
(36) Debnath, T.; Maity, P.; Ghosh, H. N. Super Sensitization: Grand Charge (Hole/Electron) Separation in Aurin Tricarboxylic Acid (ATC) Dye Sensitized CdSe Quantum Dot, CdSe/ZnS Type-I and CdSe/CdTe Type-II Core-Shell Quantum Dot Materials. *Chem.—Eur. J.* **2014**, *20*, 10.1002/chem.201403267.
(37) Singhal, P.; Ghosh, H. N. Ultrafast Hole/Electron Transfer Dynamics in CdSe Quantum Dot Sensitized by Pyrogallol red (PGR): A Super-Sensitization System. *J. Phys. Chem. C* **2014**, *118*, 16358−16365.
(38) Mora-Sero, I.; Bisquert, J. Breakthroughs in the Development of Semiconductor Sensitized Solar Cells. *J. Phys. Chem. Lett.* **2010**, *1*, 3046−3052.
(39) Choi, H.; Nicolaescu, R.; Paek, S.; Ko, J.; Kamat, P. V. Supersensitization of CdS Quantum Dots with a Near-Infrared Organic Dye: Toward the Design of Panchromatic Hybrid-Sensitized Solar Cells. *ACS Nano* **2011**, *5*, 9238−9245.
(40) Choi, H.; Kamat, P. V. CdS Nanowire Solar Cells: Dual Role of Squaraine Dye as a Sensitizer and a Hole Transporter. *J. Phys. Chem. Lett.* **2013**, *4*, 3983−3991.
(41) Shalom, M.; Albero, J.; Tachan, Z.; Martínez-Ferrero, E.; Zaban, A.; Palomares, E. Quantum Dot-Dye Bilayer-Sensitized Solar Cells: Breaking the Limits Imposed by the Low Absorbance. *J. Phys. Chem. Lett.* **2010**, *1*, 1134−1138.
(42) Dooley, C. J.; Dimitrov, S. D.; Fiebig, T. Ultrafast Electron Transfer Dynamics in CdSe/CdTe Donor-Acceptor Nanorods. *J. Phys. Chem. C* **2008**, *112*, 12074−12076.
(43) O'Connor, T.; Panov, M. S.; Mereshchenko, A.; Tarnovsky, A. N.; Lorek, R.; Perera, D.; Diederich, G.; Lambright, S.; Moroz, P.; Zamkov, M. The Effect of the Charge-Separating Interface on Exciton Dynamics in Photocatalytic Colloidal Heteronanocrystals. *ACS Nano* **2012**, *6*, 8156−8165.
(44) Ramakrishna, G.; Ghosh, H. N.; Singh, A. K.; Palit, D. K.; Mittal, J. P. Dynamics of Back-Electron Transfer Processes of Strongly Coupled Triphenyl Methane Dyes Adsorbed on $TiO_2$ Nanoparticle Surface as Studied by Fast and Ultrafast Visible Spectroscopy. *J. Phys. Chem. B* **2001**, *105*, 12786−12796.
(45) Singhal, P.; Ghosh, H. N. Ultrafast Excited Dynamics of S2 and S1 States of Tri-phenyl Methane Dyes. *Phys. Chem. Chem. Phys.* **2014**, *16*, 16824−16831.